

Angular Cross-Correlation of Galaxies: A Probe of Gravitational Lensing by Large-Scale Structure

R. Moessner¹ and Bhuvnesh Jain^{1,2}

¹*Max Planck Institut für Astrophysik, Karl Schwarzschild-Str. 1, 85740 Garching, Germany*

²*Department of Physics and Astronomy, Johns Hopkins University, Baltimore, MD 21218, USA*

4 April 2018

ABSTRACT

The angular cross-correlation between two galaxy samples separated in redshift is shown to be a useful measure of weak lensing by large-scale structure. Angular correlations in faint galaxies arise due to spatial clustering of the galaxies as well as gravitational lensing by dark matter along the line-of-sight. The lensing contribution to the 2-point auto-correlation function is typically small compared to the gravitational clustering. However the cross-correlation between two galaxy samples is nearly unaffected by gravitational clustering provided their redshift distributions do not overlap. The cross-correlation is then induced by magnification bias due to lensing by large-scale structure. We compute the expected amplitude of the cross-correlation for popular theoretical models of structure formation. For two populations with mean redshifts of $\simeq 0.3$ and 1, we find a cross-correlation signal of $\simeq 1\%$ on arcminute scales and $\simeq 3\%$ on a few arcseconds. The dependence on the cosmological parameters Ω and Λ , on the dark matter power spectrum and on the bias factor of the foreground galaxy population is explored.

Key words: galaxies: clustering - cosmology: observations - gravitational lensing - large scale structure of the Universe

1 INTRODUCTION

The angular auto-correlation function of galaxies has been widely used to characterize the large-scale structure in the universe (e.g. Peebles 1980). The observed galaxy distribution is well described by a power law $\omega(\theta) \propto \theta^{-\gamma}$, with slope $\gamma \simeq 0.8$.

Gravitational lensing by large-scale structure along the line-of-sight can alter the amplitude of $\omega(\theta)$ (Gunn 1967). Lensing increases the area of a given patch on the sky, thus diluting the number density. On the other hand, galaxies too faint to be included in a sample of given limiting magnitude are brightened due to lensing and may therefore be included in the sample. The net effect, known as magnification bias, can go either way: it can lead to an enhancement or suppression of the observed number density of galaxies, depending on the slope of the number-magnitude relation. Variations in the number density which are correlated over some angular separation alter $\omega(\theta)$. Following Kaiser (1992) and Villumsen (1996), Moessner, Jain & Villumsen (1997) (henceforth, MJV) have considered the effect of nonlinear gravitational evolution and magnification bias on $\omega(\theta)$. MJV found that for faint samples with mean redshift $z \simeq 1$ lensing

contributes 5–20% of the signal, depending on the cosmological model and angular scale. Since the lensing contribution is small even for distant galaxies, it is difficult to interpret a measurement, especially since it requires knowledge of the biasing of high-redshift galaxies relative to the mass.

In this paper we explore a different statistic, the cross-correlation function of two different galaxy samples, in order to isolate the effect of magnification bias. Consider two galaxy samples with non-overlapping redshift distributions. If the minimal distance between the two samples is several 100 Mpc, the effects of gravitational clustering are negligible. The cross-correlation function in such a case is affected entirely by magnification bias, and the dominant term is provided by the lensing effect of dark matter associated with the foreground galaxy population. Cross-correlating observables affected by gravitational lensing, such as image ellipticities of galaxies at high redshift, with the positions of galaxies at lower redshift has proved to be fruitful for detecting the effect of gravitational lensing, for example in galaxy-galaxy lensing. The cross-correlation of the number density of high-redshift quasars with foreground galaxies has also been investigated observationally (Benitez & Martinez-Gonzalez 1996) and theoretically (Bartelmann 1995, Dolag

& Bartelmann 1997). The cross-correlation of magnification and shear has been studied by Kaiser (1992), Sanz, Maritz-Gonzales & Benitez (1997) and Schneider (1997), while the auto-correlation of the shear has been computed by Blandford et al. (1991), Miralda-Escude (1991), Kaiser (1992), Bernardeau, van Waerbeke and Mellier (1996) and Jain & Seljak (1997).

Section 2 provides the formalism for computing the effects of lensing and nonlinear gravitational evolution on the angular cross-correlation function of galaxies. Results for cold dark matter (CDM)-like models are given in Section 3. We provide estimates of the errors in observational estimates of the cross-correlation in Section 4 and conclude in Section 5.

2 ANGULAR CROSS-CORRELATION: FORMALISM

This section provides the formalism for computing the angular correlation function of galaxies for a given cosmological model and primordial spectrum of fluctuations for the dark matter. The intrinsic gravitational clustering as well as the effect of gravitational lensing by the dark matter along the line-of-sight are included. Since we consider the angular correlation function, only the projected quantities are observable.

We will focus on the cross-correlation of two galaxy samples, one at high redshift, $z \gtrsim 1$, called the background sample, and the other at low redshift, $z \lesssim 0.5$, called the foreground sample. We include in our computations the true correlation between galaxies belonging to the high- and the low-redshift samples due to the overlap of their redshift distributions. As the overlap in the two redshift distributions decreases, this intrinsic clustering decreases. The effect we wish to isolate is the apparent clustering induced by gravitational lensing via magnification bias.

Let $n_1(\hat{\phi})$ be the number density of galaxies belonging to the sample with a low mean redshift $\langle z_1 \rangle$, observed in the direction $\hat{\phi}$ in the sky, and $n_2(\hat{\phi})$ that of the sample with a higher mean redshift $\langle z_2 \rangle > \langle z_1 \rangle$. The angular cross-correlation function is then defined as

$$\omega(\theta) = \langle \delta n_1(\hat{\phi}) \delta n_2(\hat{\phi}') \rangle, \quad (1)$$

where

$$\delta n_i(\hat{\phi}) \equiv \frac{n_i(\hat{\phi}) - \bar{n}_i}{\bar{n}_i} \quad (2)$$

and \bar{n}_i is the average number density of the i th sample. The fluctuation δn_i arises due to the true clustering of galaxies $\delta n_i^g(\hat{\phi})$, and due to magnification bias $\delta n_i^\mu(\hat{\phi})$,

$$\delta n_i(\hat{\phi}) = \frac{n_i(\hat{\phi}) - \bar{n}_i}{\bar{n}_i} = \delta n_i^g(\hat{\phi}) + \delta n_i^\mu(\hat{\phi}). \quad (3)$$

The goal of this paper is to compute the cross-correlation $\omega(\theta)$ arising from these two effects.

For simplicity we assume a linear bias model where galaxies trace the underlying dark matter fluctuations,

$$\delta_g(\vec{x}) = b \delta(\vec{x}). \quad (4)$$

The fluctuations on the sky due to intrinsic clustering are a projection of the density fluctuations along the line-of-sight,

weighted with the bias factor and the radial distribution $W(\chi)$ of the galaxies

$$\delta n_i^g(\hat{\phi}) = b_i \int_0^{\chi_H} d\chi W_i(\chi) \delta(r(\chi)\hat{\phi}, a). \quad (5)$$

The metric, the comoving radial coordinate χ and the comoving angular diameter distance $r(\chi)$ are introduced in the Appendix. We assume for simplicity a constant bias factor independent of scale and redshift for each galaxy population.

To determine the fluctuation due to magnification bias consider the logarithmic slope s of the number counts of galaxies $N_0(m)$ in a sample with limiting magnitude m (see MJV for details)

$$s = \frac{d \log N_0(m)}{dm}. \quad (6)$$

Magnification by amount μ changes the number counts to (e.g. Broadhurst, Taylor & Peacock 1995)

$$N'(m) = N_0(m) \mu^{2.5s-1}. \quad (7)$$

In the weak lensing limit the magnification is $\mu = 1 + 2\kappa$, where the convergence κ is a weighted projection of the density field along the line-of-sight (see equation 9 below). Since $\kappa \ll 1$ for weak lensing, equation 7 for the number counts reduces to

$$N'(m) = N_0(m) [1 + 5(s - 0.4)\kappa]. \quad (8)$$

Using $g(\chi)$ to denote the radial weight function (e.g. Jain & Seljak 1997) the convergence κ is

$$\kappa_i(\hat{\phi}) = \frac{3}{2} \Omega_m \int_0^{\chi_H} d\chi g_i(\chi) \frac{\delta(r(\chi)\hat{\phi}, a)}{a}. \quad (9)$$

The expression for $g(\chi)$ in terms of the $r(\chi)$ is given in the Appendix.

Finally, using the above relations we can re-write equation 3 for $\delta n_i(\hat{\phi})$ as

$$\delta n_i(\hat{\phi}) = \int_0^{\chi_H} d\chi f_i(\chi) \delta(r(\chi)\hat{\phi}, a), \quad (10)$$

with

$$f_i(\chi) = b_i W_i(\chi) + 3 \Omega_m (2.5s_i - 1) \frac{g_i(\chi)}{a}. \quad (11)$$

Inserting the above two equations into Eq. 1, using the small-angle approximation $\theta \ll 1$, and assuming that the radial weight functions $f_i(\chi)$ vary slowly compared to the scale of density perturbations of interest gives (Villumsen 1996),

$$\begin{aligned} \omega(\theta) &= 4\pi^2 \int_0^{\chi_H} d\chi f_1(\chi) f_2(\chi) \\ &\times \int_0^\infty dk k P(\chi, k) J_0[kr(\chi)\theta] \delta(r(\chi)\hat{\phi}, a). \end{aligned} \quad (12)$$

The power spectrum of dark matter fluctuations $P(\chi, k)$ is defined by

$$\langle \delta(\vec{k}) \delta^*(\vec{k}') \rangle = (2\pi)^6 P(\chi, k) \delta(\vec{k} - \vec{k}'). \quad (13)$$

The angular cross-correlation function is composed of four terms. In the case of $\langle z_2 \rangle > \langle z_1 \rangle$, these terms are

$$\begin{aligned} \omega(\theta) &= \langle \delta n_1^g(\hat{\phi}) \delta n_2^g(\hat{\phi}') \rangle + \langle \delta n_1^g(\hat{\phi}) \delta n_2^\mu(\hat{\phi}') \rangle \\ &+ \langle \delta n_1^\mu(\hat{\phi}) \delta n_2^\mu(\hat{\phi}') \rangle + \langle \delta n_1^\mu(\hat{\phi}) \delta n_2^g(\hat{\phi}') \rangle. \end{aligned} \quad (14)$$

The first term is due to the intrinsic clustering of the galaxies of the two samples where their redshift distributions overlap,

$$\begin{aligned} \omega_{gg}(\theta) &= b_1 b_2 4\pi^2 \int_0^{\chi_H} d\chi W_1(\chi) W_2(\chi) \\ &\times \int_0^\infty dk k P(\chi, k) J_0[kr(\chi)\theta] . \end{aligned} \quad (15)$$

Ideally we would like this term to be zero, in order to distinguish the contribution due to lensing more clearly. This could be achieved by obtaining photometric redshifts for the galaxies, and selecting two galaxy populations which do not overlap in their redshift distributions. The cross-correlation of two such samples minimizes the contribution due to intrinsic clustering, which removes uncertainties in the predictions due to unknown physical evolution of the galaxies.

The second term in equation 14 is due to the lensing of the background galaxies by the dark matter in front of it, which is traced by the foreground galaxies. The correlation thus induced between galaxies in the two samples is given by,

$$\begin{aligned} \omega_{gl}(\theta) &= b_1 3\Omega_m (2.5s_2 - 1) 4\pi^2 \int_0^{\chi_H} d\chi W_1(\chi) \frac{g_2(\chi)}{a} \\ &\times \int_0^\infty dk k P(\chi, k) J_0[kr(\chi)\theta] . \end{aligned} \quad (16)$$

The third term is due to dark matter in front of both of the galaxy samples doing the lensing. The fourth is due to dark matter traced by the background galaxies lensing the foreground galaxies. It is non-zero only if there is an overlap in the redshift distributions of the two samples. For all cases of interest these two terms are negligible compared to the second term, ω_{gl} .

2.1 Dependence on the cosmological model

Equation 15 shows how $\omega(\theta)$ depends linearly on Ω_m , aside from the dependences on Ω_m and Ω_Λ contained in the line-of-sight integral. These arise from two sources: (i) the distance factors contained in J_0 , $g(\chi)$ and $W(\chi)$, and (ii) the growth and amplitude of the power spectrum. In the linear regime, $P(\chi, k)$ depends on the linear growing mode of density perturbations $D(\chi)$ and the normalization σ_8 (which in turn can depend on the cosmological parameters) as

$$P(\chi, k) \sim [\sigma_8 D(\chi)]^2 . \quad (17)$$

The linear growing mode is well approximated by (Carroll, Press & Turner 1992)

$$\begin{aligned} D(\chi) &= \frac{5}{2} a \Omega(a) [\Omega(a)^{4/7} - \lambda(a) \\ &+ (1 + \Omega(a)/2)(1 + \lambda(a)/70)]^{-1} , \end{aligned} \quad (18)$$

where we have defined, following Mo, Jing & Börner (1996), the time dependent fractions of density in matter and vacuum energy, $\Omega(a)$ and $\lambda(a)$ in terms of the present-day values Ω_m and Ω_Λ ,

$$\Omega(a) = \frac{\Omega_m}{a + \Omega_m(1-a) + \Omega_\Lambda(a^3 - a)} \quad (19)$$

and

$$\lambda(a) = \frac{a^3 \Omega_\Lambda}{a + \Omega_m(1-a) + \Omega_\Lambda(a^3 - a)} . \quad (20)$$

Moreover, the spatial geometries differ in different models, leading to a dependence of the angular distance $r(\chi)$ on Ω_m and Ω_Λ according to Eq. 27.

The redshift distribution of galaxies can be modelled by

$$n(z) = \frac{\beta z^2}{z_0^3 \Gamma[3/\beta]} \exp[-(z/z_0)^\beta] , \quad (21)$$

for $\beta = 2.5$, which agrees reasonably well with the redshift distribution estimated for the Hubble deep field from photometric redshifts (Mobasher et al. 1996). The mean redshift is then given by

$$\langle z \rangle = \frac{\Gamma(4/\beta)}{\Gamma(3/\beta)} z_0 . \quad (22)$$

The four different cosmological models we consider are a flat universe with $\Omega_m = 1$, an open model with $\Omega_m = 0.3$, and a flat Λ -dominated model, with $\Omega_m = 0.3$ and $\Omega_\Lambda = 0.7$. These three models are normalized to cluster abundances (White, Efstathiou & Frenk 1993; Viana & Liddle 1995; Ecke, Cole & Frenk 1996; Pen 1996),

$$\sigma_8 \simeq 0.6 \Omega_m^{-0.6} . \quad (23)$$

(For $\Omega_m = 0.3$, we use $\sigma_8 = 1$, which is close to the results of the approximate formula given above.) Our fourth model is a flat universe, $\Omega_m = 1$, with a high normalization of $\sigma_8 = 1$.

The nonlinear power spectrum is obtained from the linear one through the fitting formulae of Jain, Mo & White (1995) for $\Omega_m = 1$, and from those of Peacock & Dodds (1996) for the open and Λ -dominated models. These fitting formulae are based on the idea of relating the nonlinear power spectrum at scale k to the linear power spectrum at a larger scale k_L , where the relation $k(k_L)$ depends on the power spectrum itself (Hamilton et al. 1991). They have been calibrated from and tested extensively against N-body simulations. For the linear power spectrum we take a CDM-like spectrum with shape parameter $\Gamma = 0.25$, which provides a good fit to observations. The transfer function for the initially scale-invariant power spectrum is taken from Bardeen et al. (1992).

3 CROSS-CORRELATION FUNCTION FOR CDM-LIKE POWER SPECTRA

For samples not overlapping in their redshift distributions, the cross-correlation ω_{gl} induced by lensing dominates the contribution to the cross-correlation function. The signal due to intrinsic clustering is negligibly small, though if the redshift distributions overlap significantly, it would swamp the lensing signal. In this section we present results on the cross-correlation of two galaxy samples with non-overlapping redshift distributions.

We computed $\omega_{gl}(\theta = 1')$ for two populations with mean redshifts of 0.3 and 1.5 using the redshift distribution $n(z)$ of Eq. 21. We found that the results differ by 5 – 10% from those obtained using a delta-function redshift distribution. Therefore we will use the simpler form of a delta-function distribution for computing $\omega_{gl}(\theta)$. For calculating contributions due to intrinsic clustering, however, it is necessary to use the full $n(z)$ of Eq. 21. We do this in Section 4 below to estimate the relative error made by misidentifying background galaxies as foreground ones.

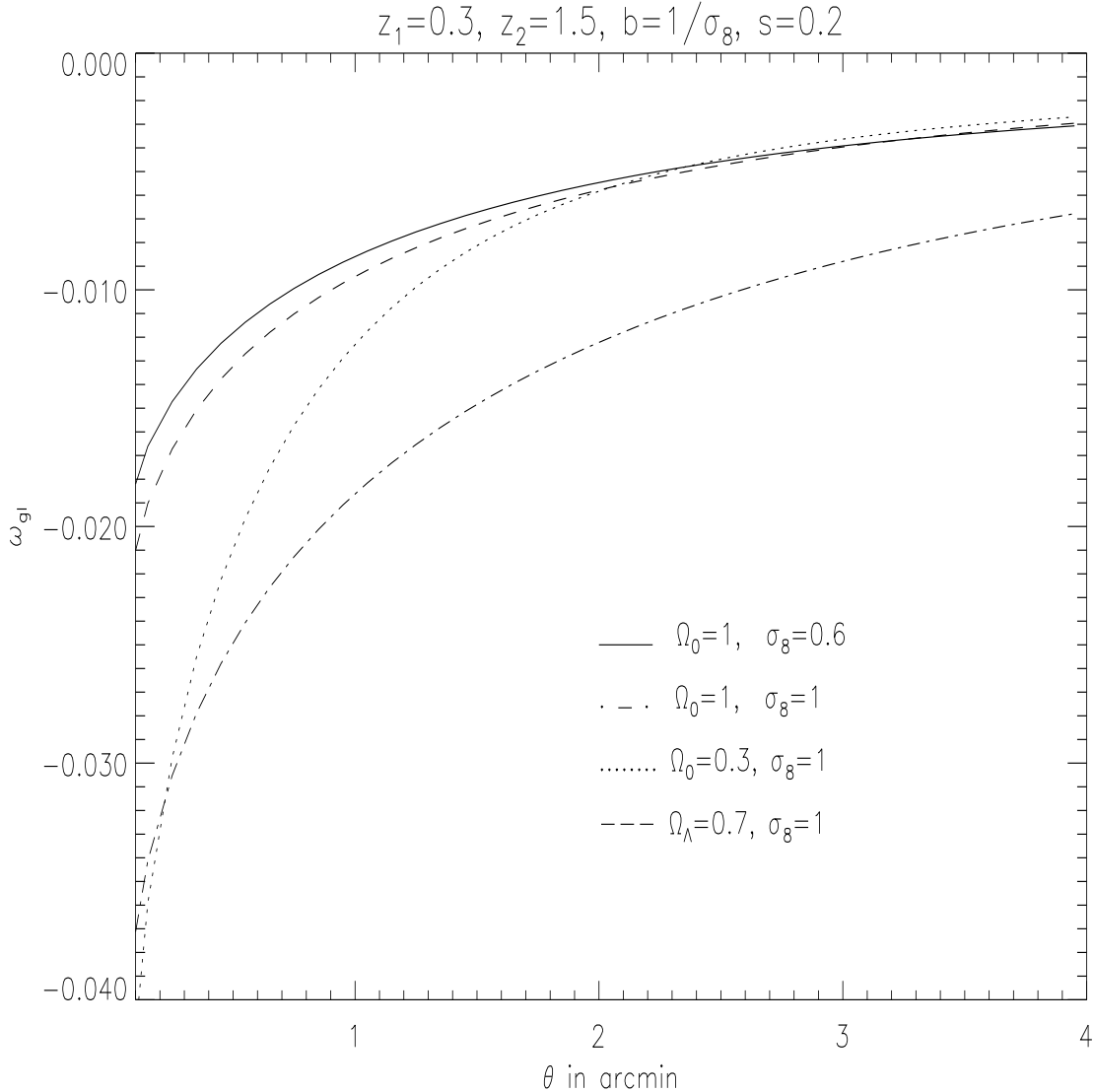


Figure 1. The cross-correlation function ω_{gl} as a function of θ is shown for the four cosmological models. Since the number count slope $s = 0.2$, magnification bias induces an anti-correlation between the foreground and background sample. Hence the sign of ω_{gl} is negative. The differences between the four models are discussed in the text.

In Figure 1 we plot ω_{gl} as a function of θ for a foreground galaxy sample at $z_1 = 0.3$ and a background sample at $z_2 = 1.5$, for the four cosmological models described in section 2.1. We choose a bias factor of $b = 1/\sigma_8$, which is in agreement with large-scale galaxy clustering data; ω_{gl} is proportional to b . We assume a number count slope of $s = 0.2$ for the background sample. For $s < 0.4$ the induced correlations are negative since $\omega_{gl}\omega_{gl} \propto (s - 0.4)$. This linear relation also makes it simple to scale our results to other values of s . A sample with a slope close to 0.2 may be obtained by defining color selected subsamples, using the fact that the number count slope is a decreasing function of $V - I$ color (Villumsen, Freudling & da Costa 1996; Broadhurst et al. 1997). The price of selecting a subsample is a smaller number of galaxies and therefore larger Poisson errors; so in practice a careful cut suited to the available data would need to be made.

Figure 1 shows that the typical cross-correlation signal expected on sub-arcminute scales is a few percent. On angular scales larger than 1 arcminute the signal drops to less than a percent. For fixed σ_8 it is largest for the Einstein-de Sitter model and smallest for the cosmological constant model, at least on arcminute scales or smaller. However if σ_8 is determined from cluster-abundances, the cross-correlation on small scales is largest for the open model.

The dependence of the cross-correlation on the redshift of the background sample is shown in Figure 2. We have plotted the cross-correlation function $\omega_{gl}(\theta = 0.1')$ for a foreground galaxy sample at $z_1 = 0.3$ as a function of the redshift z_2 of the background sample. Figure 3 is the same as Figure 2, but for $\theta = 0.2'$. These figures show the slow increase in the amplitude of the signal with $\langle z_2 \rangle$ above a redshift of 1. There is no significant variation in the shape of the curves among the four cosmological models. Thus if

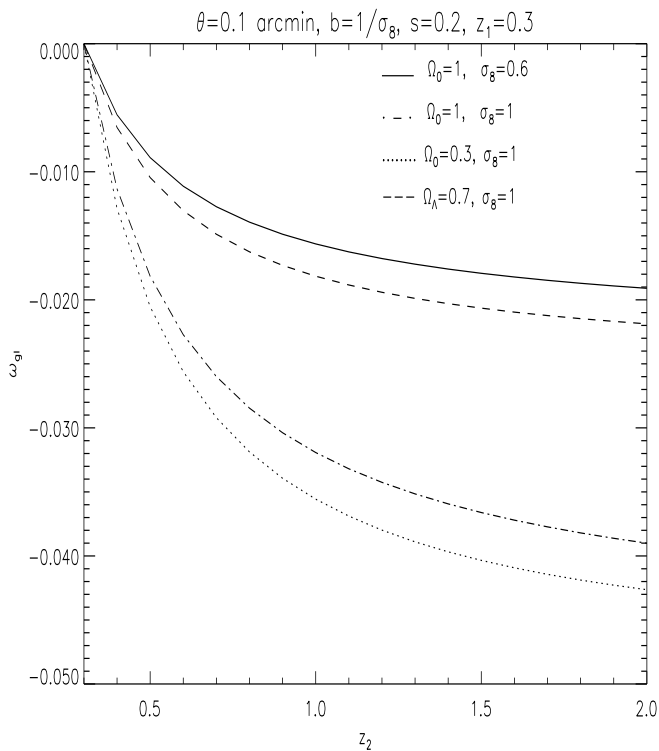


Figure 2. Cross-correlation function as a function of z_2 is shown for $z_1 = 0.3$ at $\theta = 0.1'$ for the four cosmological models. The negative correlations induced by magnification bias become stronger with z_2 , but do not change much beyond a redshift of 1.

the amplitudes were normalized to the same value at $z_2 \simeq 1$, there would be very little difference between the curves at higher z_2 .

The difference between the predictions of the four models shown in Figures 1-3 can be qualitatively understood as follows. The dominant dependence arises due to the factor of Ω_m outside the integral in equation 16 for ω_{gl} . Taking the normalization of the power spectrum into account this is reduced to $\Omega_m^{0.4}$ for the cluster-abundance normalization of σ_8 and the bias relation $b = 1/\sigma_8$. This is because the expression for ω_{gl} depends explicitly on the factor $b\Omega_m\sigma_8^2$.

The line-of-sight integral in equation 16 further weakens the dependence on Ω_m . In a low- Ω_m universe, the growth of perturbations is slowed down at late times. Hence, normalizing to present-day cluster abundances leads to a higher normalization at earlier times compared to the $\Omega_m = 1$ models. This in turn means that nonlinear effects, which are significant on angular scales of $1'$ or less, become important earlier on and lead to a larger enhancement due to nonlinear clustering by today. The nonlinear enhancement is reinforced by a geometrical effect: for lower Ω_m , and even more so for larger Ω_Λ (for given Ω_m), the physical distance to a given redshift is larger. This leads to a larger lensing path-length and thus a further increase in the lensing signal.

The combination of all these effects is shown in Figure 1. On scales well below an arcminute the signal for the open model becomes comparable to that in the Einstein-de Sitter model. This is due to the dominance of the nonlinear enhancement on these scales. The curve for the open model

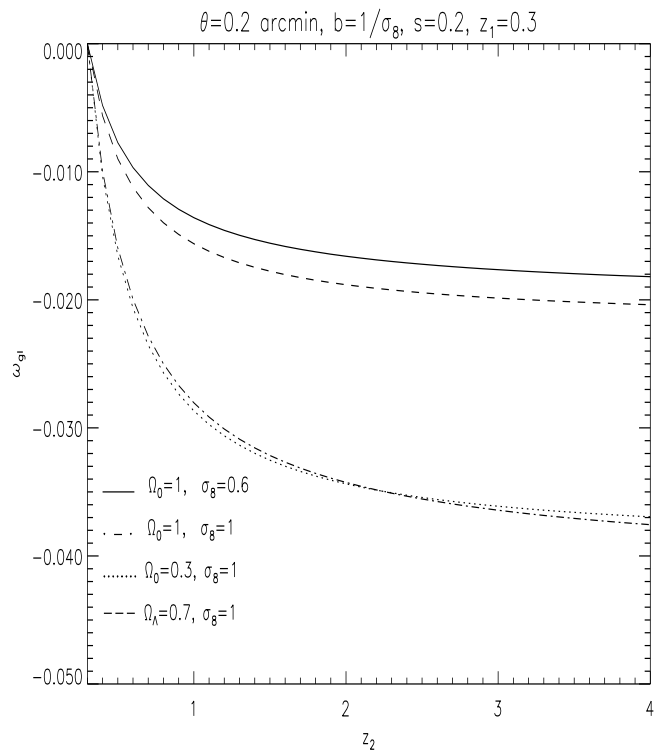


Figure 3. Cross-correlation function as a function of z_2 is shown for $\theta = 0.2'$ for the four cosmological models. All parameters except θ are as in the previous figure.

is also distinctly steeper than for the others. For $\theta > 2'$, however, there is no significant variation in the shape of the curves. For the Λ -dominated model the effect of the growing mode is not as strong as for the open model. Thus on small scales, even though the geometric effect gives a stronger enhancement than for the open model, the net amplitude of ω_{gl} is smaller than for the open model.

Finally, note that ω_{gl} is proportional to the bias factor of the foreground sample. If this bias factor is larger or smaller than the value of $b = 1/\sigma_8$ which we assumed to fit the large-scale structure data, ω_{gl} will be correspondingly altered.

4 ESTIMATE OF ERRORS

We consider two sources of error involved in an observational determination of the cross-correlation from two galaxy samples. The first potential error arises when a background galaxy is mis-identified as a foreground galaxy. In this case the auto-correlation of the background galaxy sample will erroneously enter into the measured cross-correlation. Say $\epsilon\%$ of the background galaxies' redshifts are sufficiently mis-estimated that they are taken to be part of the foreground sample. The observed cross-correlation is then given by

$$\omega_m = \omega_{gl} + \epsilon \frac{N_2}{N_1} \omega_{gg}(z_2), \quad (24)$$

where the second term is the error made due to assigning galaxies to the wrong sample. It is proportional to the fraction of galaxies which is mis-identified and to $\omega_{gg}(z_2)$, the auto-correlation function evaluated at the mean redshift

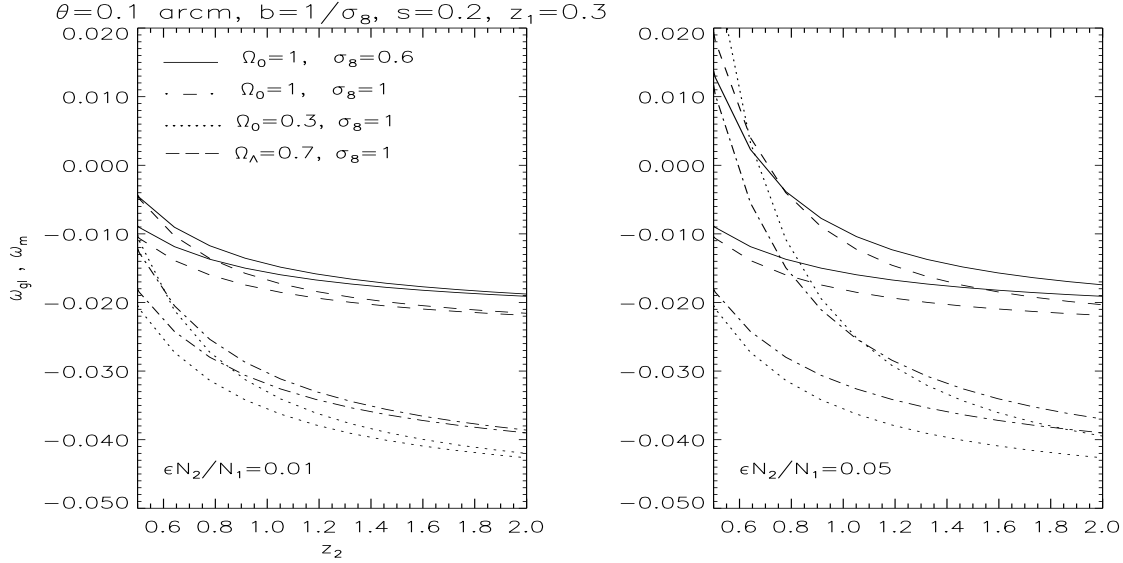


Figure 4. True cross-correlation function ω_{gl} (lower set of matching curves) and measured cross-correlation function ω_m (upper set of matching curves) when $\epsilon\%$ of the background galaxies are misidentified as foreground ones, as a function of z_2 , for $\theta = 0.1'$, $z_1 = 0.3$ and the four cosmological models.

of the background sample, for the redshift distribution of Eq. 21. We have calculated the auto-correlation at $1'$ and scaled it to $0.1'$ assuming a power law slope of -0.8 ; N_1 and N_2 are the number of galaxies in the foreground and background samples.

In Figure 4 we plot the cross-correlation $\omega_{gl}(\theta = 0.1')$ (lower set of matching curves) together with the measured cross-correlation function ω_m (upper set of matching curves). Two values of ϵ , 1% and 5% are used (for samples of equal size). The results show that for $z_2 > 1$ the error is small for $\epsilon = 1\%$ but not when $\epsilon = 5\%$. This sets an approximate standard required for using photometric redshifts or other possible methods to select the two galaxy samples.

A second source of error is the statistical uncertainty in estimating the angular correlations. Using a Poisson distribution to estimate the error in ω provides a rough guide for the number of galaxies required to estimate the cross-correlation signal. The standard deviation $\delta\omega(\theta)$ in the estimate of $\omega(\theta)$ for a random distribution of objects is given by (Peebles 1980)

$$\delta\omega(\theta)^2 = \frac{1}{N_1 N_2} \frac{\Omega}{\delta\Omega} \quad (25)$$

where Ω is the solid angle subtended by the survey area, and $\delta\Omega$ is the fraction in the bin used for angle θ . Note that $\delta\omega^2$ is just the inverse of the number of pairs in a given bin in θ .

For a sample with about 10^3 galaxies per 0.01 degree² (e.g. as in each field of Woods & Fahlman (1997) whose sample reaches limiting magnitudes of $V \sim 25$, $R \sim 25$, $I \sim 24$), the above estimate gives $\delta\omega \simeq 4 \times 10^{-3}$ if 10 bins in θ are used. Thus in excess of about 10^3 galaxies each in the foreground and background sample would be required for a detection of a $\gtrsim 1\%$ cross-correlation signal with a high level of significance.

5 CONCLUSIONS

We have presented results for the cross-correlation of two galaxy samples with different redshift distributions. The signal is dominated by the effect of magnification bias due to weak lensing. To ensure that the contribution from gravitational clustering of the galaxies is negligible, we have assumed that the redshift distributions of the two samples do not overlap. With the use of photometric redshifts (e.g. Connolly et al. 1995; Sawicki, Lin & Yee 1997), it is feasible to obtain deep galaxy samples that can be separated into sub-samples with desired redshift distributions. If only limiting magnitudes are used to create two sub-samples, then there will be a significant overlap and the interpretation of the signal is not as clean. Theoretical predictions can however be made for the expected signal assuming a redshift distribution.

The results shown in Figures 1-3 demonstrate that most models predict a signal of 1-4% for the cross-correlation function. These numbers apply for a background sample with a mean redshift $\gtrsim 1$ and a number count slope of 0.2, on angular scales from a few arcseconds to an arcminute. As argued in section 4, the measurement of such a signal appears feasible in the near future.

The cross-correlation function is a measure of the projected dark matter power spectrum. For a given spectrum, the variation with angle on small scales is largest for open cosmological models and thus provides a probe of Ω . The cross-correlation however is also proportional to the bias factor of the foreground ($z \simeq 0.3 - 0.5$) galaxy sample. Thus there is a degeneracy in the dependence on the cosmological model and the biasing of intermediate redshift galaxies. The bias factor can vary with the redshift of the foreground sample and with Ω . Given a model or empirical measure of the bias factor, the cross-correlation can be used as a probe of the power spectrum and Ω . Else, for a given cosmology, it can constrain the bias factor of galaxies. Ideally,

by combining the cross-correlation with other lensing measures which are independent of bias, such as the ellipticity auto-correlation function, constraints on the cosmological model as well as on the biasing of galaxies at intermediate redshifts can be obtained.

ACKNOWLEDGEMENT

We are grateful to Simon White for many helpful suggestions. We would like to thank Matthias Bartelmann, Andrew Connolly, Peter Schneider, Alex Szalay and Jens Villumsen for stimulating discussions. The paper also benefitted from helpful comments by the referee, Andrew Taylor.

APPENDIX A: NOTATION

Following the notation of Jain & Seljak (1997) we introduce the unperturbed metric

$$ds^2 = a^2(\tau) (-d\tau^2 + d\chi^2 + r^2(d\theta^2 + \sin^2\theta d\phi^2)), \quad (26)$$

with τ being conformal time, and χ the radial comoving distance. χ_H is used to denote the distance to the horizon. The comoving angular diameter distance $r(\chi)$ is,

$$r(\chi) = \sin_K \chi \equiv \begin{cases} K^{-1/2} \sin K^{1/2} \chi, & K > 0 \\ \chi, & K = 0 \\ (-K)^{-1/2} \sinh(-K)^{1/2} \chi, & K < 0 \end{cases} \quad (27)$$

where K is the spatial curvature given by $K = -H_0^2(1 - \Omega_m - \Omega - \Lambda)$ with H_0 being the Hubble parameter today.

With $W(\chi)$ denoting the radial distribution of galaxies in the sample, the radial weight function $g(\chi)$ is given by

$$g(\chi) = r(\chi) \int_{\chi}^{\chi_H} \frac{r(\chi' - \chi)}{r(\chi')} W(\chi') d\chi'. \quad (28)$$

For a delta-function distribution of galaxies, $W(\chi') = \delta_D(\chi' - \chi_S)$, and $g(\chi)$ reduces to $g(\chi) = r(\chi)r(\chi_S - \chi)/r(\chi_S)$.

REFERENCES

- Bardeen, J. M., Bond, J. R., Kaiser, N., & Szalay, A. S., 1986, ApJ, 304, 15
 Bartelmann, M., 1995, A & A, 298, 661
 Benitez, N., & Martinez-Gonzales, E., 1996, astro-ph/9609183
 Bernardeau, F., van Waerbeke, L., & Mellier, Y. 1996, astro-ph/9609122
 Blandford, R., Saust, A., Brainerd, T., & Villumsen, J., 1991, MNRAS, 251, 600
 Broadhurst, T. Taylor, A., & Peacock, J., 1995, ApJ, 438,49
 Broadhurst, T., Villumsen, J., Smail, I., & Charlot, S., 1997, in preparation
 Carroll, J., Press, W., & Turner, E., 1992, ARAA, 30, 499
 Connolly, A. J., Scabai, I., Szalay, A. S., Koo, D. C., Kron, R. C., & Munn, J. A., AJ, 110, 2655
 Dolag, K. & Bartelmann, M., 1997, astro-ph/9704217
 Eke, V. R., Cole, S., & Frenk, C. S. 1996, astro-ph/9601088
 Gunn, J. E. 1967, ApJ, 147, 61
 Hamilton, A. J. S., Kumar, P., Lu, E., & Matthews, A. 1991, ApJ, 374, L1
 Jain, B., Mo, H., & White, S. D. M., 1995, MNRAS, 276, L25

- Jain, B., & Seljak, U., 1997, ApJ, 484, 560
 Kaiser, N. 1992, ApJ, 388, 272
 Kaiser, N. 1996, astro-ph/9610120
 Miralda-Escude, J. 1991, ApJ, 380, 1
 Mo, H., Jing, Y.-P., & Börner, G., astro-ph/9607143.
 Mobasher, B., Rowan-Robinson, M., Georgakakis, A., & Eaton, N., 1996, MNRAS, 282, 7
 Moessner, R., Jain, B., & Villumsen, J., 1997, astro-ph/9708271
 Peacock, J., & Dodds, S., 1996, MNRAS, 218, L19.
 Peebles, P. J. E., 1980, The Large-Scale Structure of the Universe (Princeton: Princeton University Press)
 Pen, U. 1996, astro-ph/9610147.
 Sanz, J. L., Martinez-Gonzalez, E., & Benitez, N. 1997, astro-ph/9706278
 Sawicki, M. J., Lin, H., & Yee, H. K. C. 1997, AJ, 113, 1
 Schneider, P. 1997, astro-ph/9708269
 Viana, P. T. P., & Liddle, A. R. 1995, astro-ph/9511007
 Villumsen, J. 1996, MNRAS, *submitted*
 Villumsen, J., Freudling, W., & da Costa, L. 1997, ApJ, 481, 578
 Woods, D. & Fahlman, G. G. 1997, astro-ph/9707127
 White, S. D. M., Efstathiou, G., & Frenk, C. S. 1993, MNRAS, 262, 1023